Macromolecules **2008**, *41*, 2759−2761

Rapid Directed Assembly of Block Copolymer Films at Elevated Temperatures

Adam M. Welander,[†] Huiman Kang,[†] Karl O. Stuen,[†] Harun H. Solak,[‡] Marcus Müller,[§] Juan J. de Pablo,[†] and Paul F. Nealey*[,†]

Department of Chemical and Biological Engineering, University of Wisconsin, Madison, Wisconsin 53706; Laboratory for Micro- and Nanotechnology, Paul Scherrer Institute, Villigen PSI, Switzerland; and Institut für Theoretische Physik, Georg-August Universität, 37077 Göttingen, Germany

Received January 9, 2008
Revised Manuscript Received February 14, 2008

As the field of block copolymer lithography[1–8] enters its second decade of existence, the technology is moving out of the laboratory and into practice.[9] Recently, IBM announced the “first-ever application of a breakthrough self-assembling nanotechnology to conventional chip manufacturing”[10] with the introduction of their “Airgap” insulator. To enable a broader range of applications, important and active research areas are focusing on improved order, perfection, critical dimension control, feature roughness, and, additionally for practical manufacturing, the time frame for assembly. In this research we demonstrate that the time required for assembly of block copolymer films relates to polymer diffusivity and that, at accessible temperatures, mobility is such that the directed assembly of useful morphologies can occur in minutes or even seconds.

We used chemical nanopatterns to direct the assembly of the block copolymer domains into parallel lines of arbitrary length,[11] as shown in Figure 1a. We created the chemical nanopatterns using extreme ultraviolet interference lithography, as described previously,[12] with pattern periods (L_S) ranging from 40.0 to 50.0 nm, in 2.5 nm increments. This range of L_S spanned the polystyrene-*block*-poly(methyl methacrylate) (PS-*b*-PMMA) (104 kg/mol) bulk lamellar period, L_0, of 48 nm. Thin films of 55 nm thick PS-*b*-PMMA were deposited and annealed on a hot plate in a nitrogen glovebox for periods of 1 min to 3 h. When L_0 was commensurate with L_S, the time required for defect-free assembly, defined herein as lamellar structures with no disclination or dislocation defects over a 5 μm × 5 μm region representative of the total 80 μm × 200 μm patterned area, was highly dependent on the annealing temperature, as shown in Figure 1b. At a temperature of 250 °C, the annealing time needed for perfection was at most 1 min, the minimum annealing time tested, whereas at 190 °C, perfect assembly was achieved only after annealing for 50 min or longer.

Previously, Harrison et al. demonstrated that by increasing the annealing temperature of parallel-orientated cylindrical forming films of polystyrene-*block*-polyisoprene from 140 to 170 °C, they could increase the orientational correlation length (ξ) from 180 to 500 nm.[13] In their experiments, ξ increased by a factor of ~1.4 for every 10 °C increase in annealing temperature, but the annihilation of defects exhibited a $(\text{time})^{1/4}$ dependency and thus did not allow for generation of defect-free patterns. It may also be possible to increase mobility and decrease assembly time by using supercritical CO_2[14] or other solvents,[15] the latter having been shown to induce large grains (ξ) of ~10 μm with impressive order in a processing time of 6 h. However, the inclusion of additional system components has disadvantages in terms of complicating phase behavior of the system and, at least in the case of solvent annealing, formation of nonequilibrium structures.

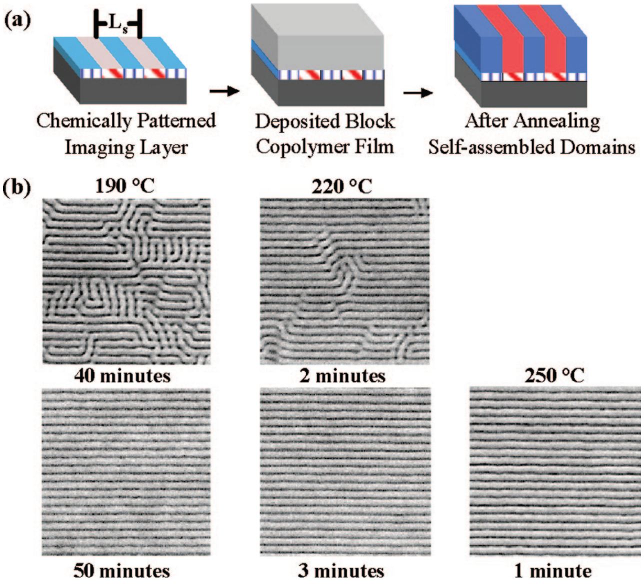

Figure 1. (a) Schematic representation of the procedure used to produce thin films of block copolymers that are directed to assemble on chemically patterned surfaces. (b) SEM micrographs of the directed assembly of PS-*b*-PMMA on chemically patterned surfaces at various annealing times and temperatures, where the chemical pattern periodicity (L_S) closely matches the natural periodicity of the block copolymer (L_0). The annealing time needed to reach perfect assembly is highly dependent on the annealing temperature. (All micrographs are 1 μm × 1 μm.)

To quantify the effect of temperature on the time frame for assembly, we annealed samples at discrete time intervals and classified them as having many or no defects from representative SEM images. This determined an upper and lower bound for the annealing time required to achieve defect-free grating structures for a range of temperatures with $L_S = L_0$. Note that at intermediate times defect-free 2 μm × 2 μm regions could be found but were not representative of the entire patterned area. This upper and lower bound can be thought of as the uncertainty in the exact annealing time needed for assembly. The linear regression of all data points in the semilog plot of annealing time vs $1/T$, shown in Figure 2, is indicative of a thermally activated process. Typically, the temperature dependence of block copolymer properties related to polymer chain mobility, including diffusivity,[16] viscosity,[17] and melt-phase moduli,[18] are modeled with the Williams−Landau−Ferry (WLF) equation.[19] The WLF equation is an empirical, two-parameter model that describes the curvature of the temperature dependence of such properties above T_g. For small ranges of T,[18,20] or for $T > T_g + 100$ °C,[21] there is typically little curvature in the T dependence of these properties, and use of an Arrhenius equation is sufficient. Hence, the block copolymer diffusivity $D(T)$ for $180 < T < 220$ °C is modeled as

---

* Corresponding author. E-mail: nealey@engr.wisc.edu.
[†] University of Wisconsin.
[‡] Paul Scherrer Institute.
[§] Georg-August Universität.

10.1021/ma800056s CCC: $40.75

$$D(T) = A\exp\left(-\frac{\Delta E_a}{RT}\right) \qquad (1)$$

where ΔE_a is the apparent activation energy of the block copolymer, A is a constant, and R is ideal gas constant. The following equation is subsequently derived to model the temperature dependence of the annealing time:

$$\ln\left(\frac{t}{t_{\mathrm{ref}}}\right) = \frac{\Delta E_a}{R}\left(\frac{1}{T} - \frac{1}{T_{\mathrm{ref}}}\right) \qquad (2)$$

where t and t_{ref} are the times required to achieve ordered structures when annealed at temperatures T and T_{ref}, respectively. The fit of eq 2 to the data shown in Figure 2 using T_{ref} = 200 °C yielded ΔE_a = 190 ± 9 kJ/mol. If the required characteristic length for diffusion and assembly is assumed to be $L_S = L_0$ = 47.5 nm, then D(190 °C) is estimated to be 7.5×10^{-15} cm^2 s^{-1}. The values of ΔE_a and D(190 °C) compare well with values in the literature for similar molecular weight block copolymers, such as for 97 kg/mol sphere forming polystyrene-*block*-poly(2-vinylpyridine) (PS-*b*-PVP), where $\Delta E_a \sim 200$ kJ/mol and D(190 °C) $\sim 6 \times 10^{-14}$ cm^2 s^{-1}.[22]

Increased polymer mobility with increasing temperature, as described above, may not be the only polymer property that changes with temperature and that impacts the assembly process. The Flory–Huggins interaction parameter, χ, and the difference in surface energy of the two blocks, $\Delta\gamma$, are also temperature-dependent. The substantial temperature dependence of χ for PS-*b*-PVP, for example, has been reported to have a large impact on order for spherical domains directed to assemble on topographic substrates.[23] However, these parameters likely do not play a large role in the PS-*b*-PMMA system. The χ parameter for PS-*b*-PMMA varies by only 4% over the range of annealing temperatures used in this study, such that the value of χN remains relatively constant in the intermediate segregation limit.[24] Since the order–disorder transition temperature (ODT) also increases in thin films,[25] we can be confident that the PS-*b*-PMMA film is well below its ODT for T < 280 °C. Regarding surface energy, it is well-known that $\Delta\gamma$ may affect the domain orientation at a free surface.[26–28] However, for the case of PS and PMMA, Wu showed that their surface energies were nearly equal from 100 to 200 °C.[29] Mansky et al. found that at 170 °C $\Delta\gamma$ for the blocks of PS-*b*-PMMA was less than 1%[30] and subsequently determined that $\Delta\gamma$ of PS and PMMA decreased with increasing temperature up to 250 °C.[31]

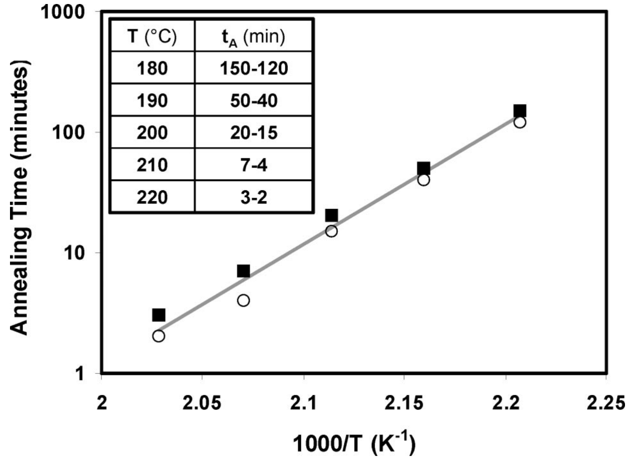

T (°C)	t_A (min)
180	150-120
190	50-40
200	20-15
210	7-4
220	3-2

Figure 2. Semilog plot of annealing time as a function of inverse temperature for (1) the minimum time observed for defect free assembly (■) and (2) the maximum time for which abundant defects still persisted (○). The line represents a linear regression of all data points with respect to eq 2 where the slope = $\Delta E_a/R$.

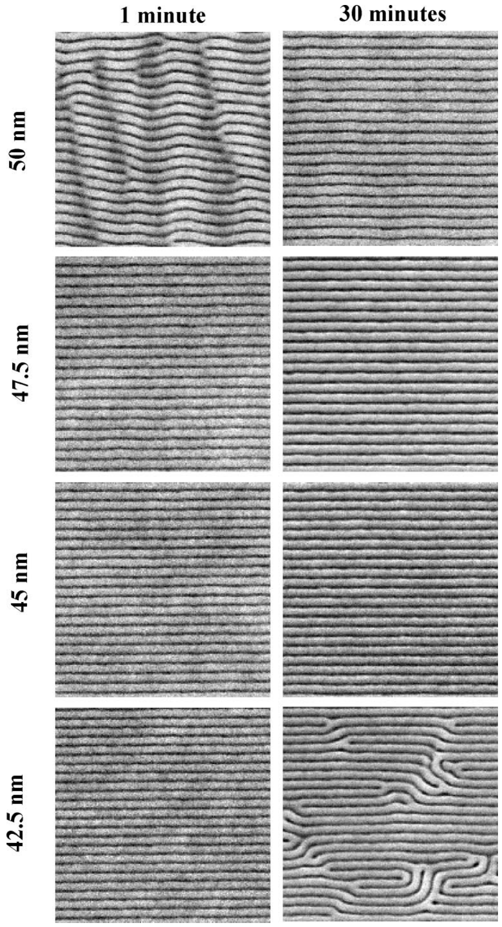

Figure 3. Top down SEM micrographs of the directed self-assembly of PS-*b*-PMMA. The lengths on the left reflect the period of the underlying chemical surface pattern (L_S), while the times on top reflect the annealing time at 280 °C. It is interesting to note that the perfectly assembled structure in the lower left most micrograph is a nonequilibrium structure. Furthermore, perfect assembly occurs a length scales much smaller than L_0 in 1 min, but at length scales larger than L_0, 30 min is required for perfection. (All micrographs are 1 μm × 1 μm.)

Extrapolation of eq 2 from the data in Figure 2 suggests that very short annealing times may be possible. For example, we would expect annealing times of 9.7 ± 2.5 and 0.9 ± 0.3 s at annealing temperatures of 250 and 280 °C, respectively. Indeed, samples annealed at 280 °C for 1 min, the minimum annealing time used in this study, displayed perfect assembly for L_S values ranging from 42.5 to 47.5 nm, as shown in Figure 3.

Interestingly, when we annealed for 30 min, the perfect assembly seen after 1 min at 280 °C for L_S of 42.5 nm degraded to form numerous defect structures, similar to defect structures observed after annealing an identical sample at 190 °C for 3 days,[12] but for L_S = 47.5 nm, the structures remained defect-free. This leads us to conclude that in this isolated case the perfect assembly observed with L_S of 42.5 nm after 1 min of annealing may have been a nonequilibrium structure. At present, the stability and mechanism of forming this nonequilibrium structure are unknown, but it is interesting to note that assembly occurs much faster when $L_S < L_0$ as compared to $L_S > L_0$.

Increased polymer mobility at higher annealing temperatures is also effective in decreasing processing time for assembly of block copolymers on chemical patterns of complex geometries[32] or on topographical substrates.[33–36] Previously, ternary blends

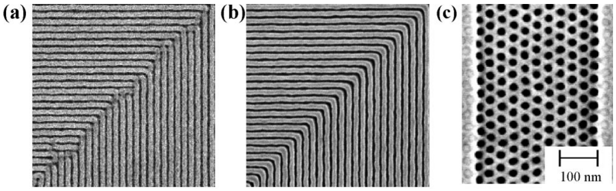

2 minutes **15 minutes** **5 minutes**

Figure 4. Top down SEM micrographs of the directed self-assembly of PS-*b*-PMMA. (a) Nonregular device structures assembled in 2 min at 250 °C. While the area with parallel lines shows perfect ordering, defects persist in the corners. The homopolymer needs more time to diffuse to the corner in order for perfection. (b) Same pattern after 15 min showing perfection in all regions. Both images are 2 μm × 2 μm. (c) Hexagonally packed cylinders assembled using graphoepitaxy, annealed at 250 °C for 5 min.

of PS-*b*-PMMA with PS and PMMA homopolymers were directed to assemble on nested bends after annealing at 190 °C for 7 days.[32] Using the same system, we can now achieve perfect directed self-assembly in 15 min of annealing at 250 °C, as shown in Figure 4b. After only 2 min of annealing, the parallel lines were assembled perfectly, as in Figure 1, but defects existed in the corners, as shown in Figure 4a, providing evidence that there was insufficient time for the homopolymers to segregate to the corners of the structures. It is this localized redistribution of the homopolymer to high-energy regions that reduces stress and facilitates perfect assembly.[32] Figure 4c shows the perfect topographical assembly after annealing for 5 min at 250 °C of cylinders in channels. The 5 min annealing time is a dramatic decrease in time compared to the literature values of 17[33] and 24 h[36] for similar systems. The assembly time is significantly longer than that of linear aligned lamellae on chemical patterns, however, due to the decrease in driving force for assembly where only the walls show preferential wetting.

In conclusion, desirable attributes for the implementation of block copolymer lithography in many applications include straightforward insertion into traditional lithographic processes, consisting of spin coating, baking, and etch steps, and process stability afforded by the assembled film representing equilibrium structures. Previous research demonstrated these attributes, but used long processing times, in part to ensure that such equilibrium structures were achieved. Here we demonstrate that by using traditional resist processing steps block copolymers can be directed to assemble into templates within a time frame comparable to postexposure bake times of traditional photoresists, while at the same time maintaining the desirable attributes for implementation in lithographic applications.

Acknowledgment. This work was supported by the Semiconductor Research Corporation (SRC) and NSF through the Nanoscale Science and Engineering Center. This work made use of the facilities and staff at the UW Center for Nanotechnology, the Synchrotron Radiation Center at UW Madison, and the Swiss Light Source at the Paul Scherrer Institute.

References and Notes

(1) Park, M.; Harrison, C.; Chaikin, P. M.; Register, R. A.; Adamson, D. H. *Science* **1997**, *276* (5317), 1401–1404.
(2) Lopes, W. A.; Jaeger, H. M. *Nature (London)* **2001**, *414* (6865), 735–738.
(3) Thurn-Albrecht, T.; Schotter, J.; Kastle, C. A.; Emley, N.; Shibauchi, T.; Krusin-Elbaum, L.; Guarini, K.; Black, C. T.; Tuominen, M. T.; Russell, T. P. *Science* **2000**, *290* (5499), 2126–2129 .
(4) Li, R. R.; Dapkus, P. D.; Thompson, M. E.; Jeong, W. G.; Harrison, C.; Chaikin, P. M.; Register, R. A.; Adamson, D. H. *Appl. Phys. Lett.* **2000**, *76* (13), 1689–1691.
(5) Cheng, J. Y.; Ross, C. A.; Chan, V. Z. H.; Thomas, E. L.; Lammertink, R. G. H.; Vancso, G. J. *Adv. Mater.* **2001**, *13* (15), 1174.
(6) Urbas, A.; Sharp, R.; Fink, Y.; Thomas, E. L.; Xenidou, M.; Fetters, L. J. *Adv. Mater.* **2000**, *12* (11), 812–814.
(7) Black, C. T.; Guarini, K. W.; Milkove, K. R.; Baker, S. M.; Russell, T. P.; Tuominen, M. T. *Appl. Phys. Lett.* **2001**, *79* (3), 409–411.
(8) Mansky, P.; Chaikin, P.; Thomas, E. L. *J. Mater. Sci.* **1995**, *30* (8), 1987–1992.
(9) Black, C. T.; Ruiz, R.; Breyta, G.; Cheng, J. Y.; Colburn, M. E.; Guarini, K. W.; Kim, H. C.; Zhang, Y. *IBM J. Res. Dev.* **2007**, *51* (5), 605–633.
(10) IBM Brings Nature to Computer Chip Manufacturing. IBM Press Release May 3, 2007.
(11) Kim, S. O.; Solak, H. H.; Stoykovich, M. P.; Ferrier, N. J.; de Pablo, J. J.; Nealey, P. F. *Nature (London)* **2003**, *424* (6947), 411–414.
(12) Edwards, E. W.; Montague, M. F.; Solak, H. H.; Hawker, C. J.; Nealey, P. F. *Adv. Mater.* **2004**, *16* (15), 1315000.
(13) Harrison, C.; Adamson, D. H.; Cheng, Z. D.; Sebastian, J. M.; Sethuraman, S.; Huse, D. A.; Register, R. A.; Chaikin, P. M. *Science* **2000**, *290* (5496), 1558–1560.
(14) RamachandraRao, V. S.; Gupta, R. R.; Russell, T. P.; Watkins, J. J. *Macromolecules* **2001**, *34* (23), 7923–7925.
(15) Kim, S. H.; Misner, M. J.; Xu, T.; Kimura, M.; Russell, T. P. *Adv. Mater.* **2004**, *16* (3), 226000.
(16) Dalvi, M. C.; Eastman, C. E.; Lodge, T. P. *Phys. Rev. Lett.* **1993**, *71* (16), 2591–2594.
(17) Chapman, B. R.; Hamersky, M. W.; Milhaupt, J. M.; Kostelecky, C.; Lodge, T. P.; von Meerwall, E. D.; Smith, S. D. *Macromolecules* **1998**, *31* (14), 4562–4573.
(18) Kotaka, T.; Okamoto, M.; Kojima, A.; Kwon, Y. K.; Nojima, S. *Polymer* **2001**, *42* (7), 3223–3231.
(19) Ferry, J. D. *Viscoelastic Properties of Polymers*, 3rd ed.; Wiley: New York, 1980.
(20) Nealey, P. F.; Cohen, R. E.; Argon, A. S. *Macromolecules* **1993**, *26* (6), 1287–1292.
(21) Bird, R. B.; Armstrong, R. C.; Hassager, O. *Dynamics of Polymer Liquids*, 2nd ed.; John Wiley & Sons: New York, 1987; Vol. *1*. (Fluid Mechanics).
(22) Yokoyama, H.; Kramer, E. J. *Macromolecules* **1998**, *31* (22), 7871–7876.
(23) Segalman, R. A.; Hexemer, A.; Hayward, R. C.; Kramer, E. J. *Macromolecules* **2003**, *36* (9), 3272–3288.
(24) Russell, T. P.; Hjelm, R. P.; Seeger, P. A. *Macromolecules* **1990**, *23* (3), 890–893.
(25) Menelle, A.; Russell, T. P.; Anastasiadis, S. H.; Satija, S. K.; Majkrzak, C. F. *Phys. Rev. Lett.* **1992**, *68* (1), 67–70.
(26) Anastasiadis, S. H.; Russell, T. P.; Satija, S. K.; Majkrzak, C. F. *Phys. Rev. Lett.* **1989**, *62* (16), 1852–1855.
(27) Liu, Y.; Zhao, W.; Zheng, X.; King, A.; Singh, A.; Rafailovich, M. H.; Sokolov, J.; Dai, K. H.; Kramer, E. J.; Schwarz, S. A.; Gebizlioglu, O.; Sinha, S. K. *Macromolecules* **1994**, *27* (14), 4000–4010.
(28) Mansky, P.; Russell, T. P.; Hawker, C. J.; Pitsikalis, M.; Mays, J. *Macromolecules* **1997**, *30* (22), 6810–6813.
(29) Wu, S. *J. Phys. Chem.* **1970**, *74* (3), 632000.
(30) Mansky, P.; Liu, Y.; Huang, E.; Russell, T. P.; Hawker, C. *Science* **1997**, *275* (5305), 1458–1460.
(31) Mansky, P.; Russell, T. P.; Hawker, C. J.; Mays, J.; Cook, D. C.; Satija, S. K. *Phys. Rev. Lett.* **1997**, *79* (2), 237–240.
(32) Stoykovich, M. P.; Muller, M.; Kim, S. O.; Solak, H. H.; Edwards, E. W.; de Pablo, J. J.; Nealey, P. F. *Science* **2005**, *308* (5727), 1442–1446.
(33) Black, C. T.; Bezencenet, O. *IEEE Trans. Nanotechnol.* **2004**, *3* (3), 412–415.
(34) Kim, S. H.; Misner, M. J.; Xu, T.; Kimura, M.; Russell, T. P. *Adv. Mater.* **2004**, *16* (3), 226–231.
(35) Sundrani, D.; Sibener, S. J. *Macromolecules* **2002**, *35* (22), 8531–8539.
(36) Xiao, S. G.; Yang, X. M.; Edwards, E. W.; La, Y. H.; Nealey, P. F. *Nanotechnology* **2005**, *16* (7), S324–S329.

MA800056S